

# Ruthenium Terpyridine Complexes Containing a Pyrrole-Tagged 2,2'-Dipyridylamine Ligand—Synthesis, Crystal Structure, and Electrochemistry

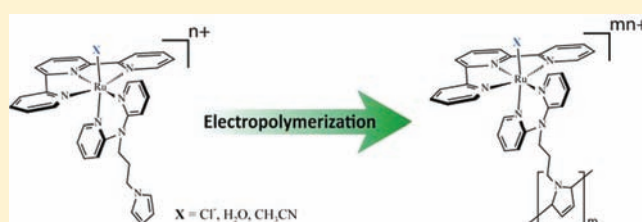
Kwong-Chak Cheung, Peng Guo, Ming-Him So, Zhong-Yuan Zhou, Lawrence Yoon Suk Lee, and Kwok-Yin Wong\*

Department of Applied Biology and Chemical Technology and the State Key Laboratory of Chirosciences, The Hong Kong Polytechnic University, Hunghom, Kowloon, Hong Kong, China

## Supporting Information

**ABSTRACT:** Ruthenium(II) terpyridine complexes containing the pyrrole-tagged 2,2'-dipyridylamine ligand PPP (where PPP stands for *N*-(3-bis(2-pyridyl)aminopropyl)pyrrole with the general formula  $[\text{Ru}(\text{tpy})(\text{PPP})\text{X}]^{n+}$  (1, X = Cl<sup>-</sup>; 2, X = H<sub>2</sub>O; 3, X = CH<sub>3</sub>CN; tpy = 2,2':6',2''-terpyridine) have been synthesized and characterized by <sup>1</sup>H NMR, IR, UV-vis, mass spectrometry, and elemental analysis. 1 and 2 have been structurally characterized by X-ray crystallography. Both 1 and 2

were successfully immobilized onto glassy carbon electrode via anodic oxidation of the pyrrole moiety on the PPP ligand to give stable and highly electroactive polymer films. Cyclic voltammetric studies of 1 in acetonitrile revealed a Ru<sup>III</sup>/Ru<sup>II</sup> couple at 0.4 V vs Cp<sub>2</sub>Fe<sup>+0</sup> initially, but another redox couple resulting from chloride substitution by acetonitrile developed at  $E_{1/2} = 0.82$  V upon repetitive potential scan. This ligand substitution was induced by the acidic local environment caused by the release of protons during pyrrole polymerization. The electropolymerization of 2 in aqueous medium allowed the observation of the formation of Ru<sup>IV</sup>=O species in polypyrrole film. As the film grew thicker, the size of the Ru<sup>III</sup>/Ru<sup>II</sup> couple ( $E_{1/2} = 0.8$  V vs SCE at pH 1) of poly[Ru(tpy)(PPP)(OH<sub>2</sub>)]<sup>n+</sup> increased accordingly, whereas the growth of the Ru<sup>IV</sup>/Ru<sup>III</sup> couple ( $E_{1/2} = 0.89$  V vs SCE at pH 1) leveled off after the film had reached a certain thickness. The Pourbaix diagram of the  $E_{1/2}$  of the Ru<sup>III</sup>/Ru<sup>II</sup> and Ru<sup>IV</sup>/Ru<sup>III</sup> couples vs pH of the electrolyte medium has been obtained. The resulting poly[Ru(tpy)(PPP)(OH<sub>2</sub>)]<sup>n+</sup> film is electrocatalytically active toward the oxidation of benzyl alcohol.



## INTRODUCTION

Modified electrode surfaces have received much attention not only because they can provide a model system for studying interfacial electron transfer<sup>1</sup> but also because they can find numerous potential applications such as electrocatalysis,<sup>2</sup> biosensors,<sup>3</sup> and molecular electronic devices.<sup>4</sup> Among the many available methods of surface modification, the electrochemical grafting of conducting polymers, such as polypyrrole, polyaniline, and polythiophene, is one of the most widely employed techniques. It offers an easy and efficient way of introducing new functionalities or altering the surface properties by entrapping molecules of interest in the polymer network and immobilizing them on the electrode surface. Particularly, pyrrole and its derivatives are well-known to undergo an oxidative electropolymerization to produce an adhesive and durable film on electrode surfaces.<sup>5</sup>

Polypyridine ligands are one of the most versatile classes of ligands in coordination chemistry and have been used as a linker for attachment of electropolymerizable units to various transition metal complexes. Use of polypyridine ligands containing electropolymerizable units such as vinyl, aniline, or pyrrole groups allows the easy incorporation of metal complexes onto electrode surfaces, and such chemically

modified electrodes have potential advantages for electrocatalysis, for example, stabilization and less use of catalyst.<sup>6</sup> Moutet and Deronzier have further developed the method by synthesizing a number of polypyridine ligands with a pyrrole pendant.<sup>7</sup> They have conducted extensive studies on the electropolymerization of the ruthenium,<sup>8</sup> rhenium,<sup>9</sup> and manganese<sup>10</sup> complexes of these ligands. However, these pyrrole-containing polypyridine ligands are difficult to synthesize, and the yields are low (<10%). Moreover, the electropolymerization of their metal complexes are often restricted to nonaqueous medium. More recently, Deronzier and co-workers have also reported the synthesis of the pyrrole-containing tridentate *N,N*-bis(2-pyridylmethyl)ethylamine and electropolymerization of its ruthenium complexes in acetonitrile or dichloromethane.<sup>11</sup>

We have recently reported the pyrrole-tagged bidentate ligand, *N*-(3-bis(2-pyridyl)aminopropyl)pyrrole (PPP), the structure of which is based on 2,2'-dipyridylamine (dpa), and its rhenium complex.<sup>12</sup> In this article, we describe the synthesis of some ruthenium terpyridine complexes of PPP and the

Received: November 15, 2011

Published: June 6, 2012

electrode surface modification with them via electropolymerization. Direct electropolymerization of the ruthenium terpyridine aquo complex of PPP in aqueous medium allowed the observation of the electrochemical formation of high valent  $\text{Ru}^{\text{IV}}=\text{O}$  species in polypyrrole film, which is considered as an exceptionally reactive electrocatalyst for multielectron oxidation of various substrates.<sup>13</sup>

## EXPERIMENTAL SECTION

**Materials.** Triethylamine ( $\geq 99.5\%$ ), ruthenium trichloride trihydrate, *N*-(2-cyanoethyl)pyrrole (97%), 2,2'-dipyridylamine (dpa, 99%), lithium aluminum hydride ( $\text{LiAlH}_4$ , 95%), 2,2':6',2''-terpyridine (tpy, 98%), 2,2'-bipyridine (bpy, 98%), sodium *tert*-butoxide (*t*-BuONa, 97%), lithium perchlorate ( $\text{LiClO}_4$ , 99%), silver trifluoromethanesulfonate ( $\geq 99\%$ ), and tetrabutylammonium perchlorate (TBAP, 98%) were purchased from Aldrich. Lithium chloride ( $\text{LiCl}$ , 99%) was purchased from Acros, and BINAP (98%, racemic) was purchased from Strem. All the chemicals were used without further purification. *N*-(3-bis(2-pyridyl)aminopropyl)pyrrole (PPP),<sup>12</sup>  $[\text{Ru}(\text{tpy})\text{Cl}_3]$ ,<sup>14</sup>  $[\text{Ru}(\text{tpy})(\text{dpa})\text{Cl}]\text{ClO}_4$ ,<sup>15</sup>  $[\text{Ru}(\text{tpy})(\text{dpa})(\text{OH}_2)](\text{ClO}_4)_2$ ,<sup>15</sup> and (2,2'-dipyridyl)propylamine (dppa)<sup>16</sup> were prepared according to the procedures previously reported in literature.

**$[\text{Ru}(\text{tpy})(\text{PPP})\text{Cl}]\text{ClO}_4$  (1).** A mixture of 330 mg of  $[\text{Ru}(\text{tpy})\text{Cl}_3]$  (0.75 mmol), 0.5 g of  $\text{LiCl}$ , 200 mg of *N*-(3-bis(2-pyridyl)aminopropyl)pyrrole (PPP, 0.75 mmol), and 1.0 mL triethylamine was gently refluxed for 2.5 h under argon in 40 mL of absolute ethanol. After the reaction mixture had been cooled down to room temperature, it was filtered to remove any insoluble material. The filtrate was concentrated to about 5 mL, and 20 mL of aqueous solution of saturated  $\text{LiClO}_4$  was added. Pale brown microcrystalline solid slowly separated out, which was collected by filtration, washed thoroughly with water and ether, and dried in a vacuum oven. Yield: 0.52 g (93%).  $^1\text{H NMR}$  ( $\text{CD}_3\text{CN}$ ,  $\delta$  ppm): 9.54 (d, 1H), 8.36 (d, 2H), 8.30 (d, 2H), 8.16 (d, 2H), 8.05 (t, 1H), 7.87 (dt, 3H), 7.36 (dt, 5H), 6.75 (d, 1H), 6.67 (d, 1H), 6.57 (s, 2H), 6.40 (t, 1H), 6.00 (s, 2H), 3.85 (t, 2H), 3.36 (t, 2H), 1.05 (t, 2H). IR (KBr pellet,  $\text{cm}^{-1}$ ): 1599 (m,  $\nu$  C=N), 1462 (s), 1486 (w), 1090 (s), 768 (m), 733 (m), 623 (m). UV-vis [ $\lambda_{\text{max}}$  nm ( $\epsilon$ ,  $\text{M}^{-1}\text{cm}^{-1}$ ) in  $\text{CH}_3\text{CN}$ ]: 226 (25600), 273 (27800), 315 (22100), 378 (br), 495 (br), 554 (br) (4000). Elemental analysis for  $\text{C}_{32}\text{H}_{29}\text{N}_7\text{Cl}_2\text{O}_4\text{Ru}$ : Calcd C, 51.4; H, 3.9; N, 13.1. Found: C, 51.8; H, 4.1; N, 13.3%. ESI-MS:  $m/z$  649 ( $\text{M} + \text{H}$ )<sup>+</sup>. Crystals suitable for X-ray diffraction study were obtained by vapor diffusion of diethyl ether into an acetonitrile solution of the complex.

**$[\text{Ru}(\text{tpy})(\text{PPP})(\text{OH}_2)](\text{CF}_3\text{SO}_3)_2$  (2).** A mixture of 0.24 g of 1 and 0.08 g of silver trifluoromethanesulfonate was gently heated for 1 h in 40 mL of 1:3 acetone–water in the dark. After cooling down to room temperature, the mixture was filtered to remove the precipitated AgCl. A total of 15 mL of saturated lithium trifluoromethanesulfonate ( $\text{CF}_3\text{SO}_3\text{Li}$ ) solution was then added to the filtrate, and the resulting mixture was chilled overnight in a refrigerator. Dark-red microcrystalline precipitate of  $[\text{Ru}(\text{tpy})(\text{PPP})(\text{OH}_2)](\text{CF}_3\text{SO}_3)_2$  was collected by filtration, washed with the minimum amount of cold water and diethyl ether, and air-dried. Yield: 0.21 g (69%).  $^1\text{H NMR}$  ( $\text{D}_2\text{O}$ ,  $\delta$  ppm): 8.81 (d, 1H), 8.40 (d, 2H), 8.34 (d, 2H), 8.20 (d, 2H), 8.05 (t, 1H), 7.99 (t, 1H), 7.90 (t, 2H), 7.42 (m, 5H), 6.8 (d, 1H), 6.73 (d, 1H), 6.64 (t, 2H), 6.32 (t, 1H), 6.08 (t, 2H), 3.8 (m, 4H), 1.3 (s, 2H). IR ( $\text{cm}^{-1}$ , KBr pellet): 3440 (m), 3093 (w), 2972 (w), 2925 (w), 1633 (w), 1600 (w), 1463 (w), 1445 (s), 1093 (s), 769 (s), 624 (m). UV-vis [ $\lambda_{\text{max}}$  nm ( $\epsilon$ ,  $\text{M}^{-1}\text{cm}^{-1}$ ) in 0.1 M  $\text{CF}_3\text{SO}_3\text{H}$ ]: 226 (20100), 273 (23300), 315 (20400), 334 (sh), 373 (sh), 508 (br) (3400). Elemental analysis for  $\text{C}_{34}\text{H}_{31}\text{F}_6\text{N}_7\text{O}_7\text{S}_2\text{Ru}$ : Calcd C, 44.0; H, 3.4; N, 10.6. Found: C, 44.3; H, 3.6; N, 10.4. ESI-MS  $m/z$ : 306 ( $\text{M} - \text{OH}_2$ )<sup>2+</sup>. Crystals suitable for X-ray diffraction study were obtained by recrystallization of the complex in 0.1 M  $\text{CF}_3\text{SO}_3\text{H}$ .

**$[\text{Ru}(\text{tpy})(\text{PPP})(\text{CH}_3\text{CN})](\text{ClO}_4)_2$  (3).** A total of 0.5 g of 2 was dissolved in 30 mL of dry  $\text{CH}_3\text{CN}$ . The mixture was gently refluxed for 30 min in the dark. After cooling down to room temperature, aqueous  $\text{LiClO}_4$  was added and the solvent was slowly removed under vacuum. The product precipitated out and was filtered off as a dark-red

microcrystalline solid. Yield: 0.46 g (90%).  $^1\text{H NMR}$  ( $\text{CD}_3\text{CN}$ ,  $\delta$  ppm): 9.06 (d, 1H), 8.47 (dt, 4H), 8.21 (t, 4H), 8.08 (t, 2H), 7.59 (m, 5H), 7.16 (m, 2H), 6.82 (t, 1H), 6.63 (d, 1H), 4.06 (dd, 3H), 3.59 (m, 2H), 3.24 (t, 2H), 1.00 (t, 2H). IR ( $\text{cm}^{-1}$ , KBr pellet): 3448 (m), 3084 (w), 2925 (w), 1466 (w), 1258 (s), 1158 (s), 1030 (s), 771 (s), 638 (m). UV-vis [ $\lambda_{\text{max}}$  nm ( $\epsilon$ ,  $\text{M}^{-1}\text{cm}^{-1}$ ) in  $\text{CH}_3\text{CN}$ ]: 226 (22300), 272 (24400), 310 (21700), 360 (sh), 473 (br) (3900). Elemental analysis for  $\text{C}_{34}\text{H}_{32}\text{N}_8\text{Cl}_2\text{O}_8\text{Ru}$ : Calcd C, 47.9; H, 3.8; N, 13.1. Found: C, 47.7; H, 3.6; N, 13.0%. ESI-MS:  $m/z$  327 ( $\text{M}$ )<sup>2+</sup>.

**$[\text{Ru}(\text{tpy})(\text{dppa})\text{Cl}]\text{ClO}_4$ .** A mixture of 330 mg of  $[\text{Ru}(\text{tpy})\text{Cl}_3]$  (0.75 mmol), 0.5 g of  $\text{LiCl}$ , 160 mg of (2,2'-dipyridyl)propylamine (dppa, 0.75 mmol), and 1.0 mL triethylamine was gently refluxed for 2.5 h under argon in 40 mL of absolute ethanol. After the reaction mixture had been cooled down to room temperature, it was filtered to remove any insoluble material. The filtrate was concentrated to about 5 mL, and 20 mL aqueous solution of saturated  $\text{LiClO}_4$  was added. Pale brown microcrystalline solid slowly precipitated out, which was collected by filtration, washed thoroughly with water and diethyl ether, and dried in a vacuum oven. Yield: 0.42 g (82%).  $^1\text{H NMR}$  ( $\text{CD}_3\text{CN}$ ,  $\delta$  ppm): 9.55 (d, 1H), 8.34 (dd, 4H), 8.21 (d, 2H), 8.07 (t, 1H), 7.91 (m, 3H), 7.55 (d, 1H), 7.40 (m, 4H), 6.69 (d, 1H), 6.69 (d, 1H), 6.41 (t, 1H), 3.89 (d, 2H), 1.04 (m, 2H), 0.82 (t, 3H). IR (KBr pellet,  $\text{cm}^{-1}$ ): 1595 (m,  $\nu$  C=N), 1462 (s), 1444 (w), 1107, (s), 1090 (w), 1081 (s), 790 (m), 765 (m), 622 (m). UV-vis [ $\lambda_{\text{max}}$  nm ( $\epsilon$ ,  $\text{M}^{-1}\text{cm}^{-1}$ ) in  $\text{CH}_3\text{CN}$ ]: 235 (23400), 275 (24200), 319 (21200), 364 (br), 486 (br), 538 (br) (5600). Elemental analysis for  $\text{C}_{28}\text{H}_{26}\text{Cl}_2\text{N}_6\text{O}_4\text{Ru}$ : Calcd C, 49.3; H, 3.8; N, 12.3. Found: C, 49.1; H, 3.8; N, 12.3. ESI-MS:  $m/z$  584 ( $\text{M} + \text{H}$ )<sup>+</sup>.

**Physical Measurements.** Cyclic voltammetric measurements were conducted using a potentiostat (CHI1030A, CH Instruments) at room temperature. A conventional three-electrode system was employed with an in-house designed two-compartment glass cell. A glassy carbon electrode (BAS M2070, surface area = 0.07  $\text{cm}^2$ ) was used as the working electrode, a Pt wire loop as the auxiliary electrode, and a Ag/AgNO<sub>3</sub> electrode as a reference electrode. Nonaqueous electrochemistry was carried out in acetonitrile or dichloromethane, which were distilled over  $\text{CaH}_2$  under nitrogen. 0.1 M TBAP was used as an electrolyte, and the reference potential was adjusted against the  $E_{1/2}$  of ferrocenium/ferrocene couple ( $\text{Cp}_2\text{Fe}^{+/0}$ ) measured in the same electrolyte. UV–visible spectra were recorded on a Milton-Roy Spectronic 3000 diode array spectrophotometer. Infrared (IR) spectra were obtained on a Bruker Vertex 70 FT-IR spectrometer.  $^1\text{H NMR}$  spectra were obtained on a Bruker DPX-400 FT-NMR spectrometer. Chemical shifts ( $\delta$  ppm) were reported relative to tetramethylsilane ( $\text{Si}(\text{CH}_3)_4$ ). Electrospray ionization mass spectra were recorded on a Finnigan mass spectrometer (MAT 95). Scanning electron microscopic (SEM) spectra were obtained on a Leica Stereoscan 440 scanning electron microscope. The samples for SEM were prepared by polymerizing the ruthenium complex onto a demountable glassy carbon disk electrode and drying the resulting polymer films under an air blower followed by sputter-coating with gold.

**X-ray Structure Determination.** The crystal structures of complexes 1 and 2 were determined by a direct method which yielded the positions of part of the non-hydrogen atoms. Subsequent difference Fourier syntheses were employed to locate all of the remaining non-hydrogen atoms which did not show up in the initial structure. All non-hydrogen atoms were refined anisotropically with the weight function

$$W = \frac{q}{\sigma^2(F_0^2) + (ap)^2 + (bp) + d + (e \sin \theta)}$$

where  $p = [f \times \max(0 \text{ or } F_0^2) + (1 - f) \times F_c^2]$ . Hydrogen atoms were located based on the difference Fourier syntheses connecting geometrical analysis. All the experiments and computations were performed on a PC with the software Bruker Smart and Bruker Shelxtl package.<sup>17</sup>

The X-ray structure data can be obtained free of charge from The Cambridge Crystallographic Data Centre via [www.ccdc.cam.ac.uk/data\\_request/cif](http://www.ccdc.cam.ac.uk/data_request/cif). CCDC 853073 and 853074 contain the supple-

mentary crystallographic data for  $[\text{Ru}(\text{tpy})(\text{PPP})\text{Cl}]\text{ClO}_4$  and  $[\text{Ru}(\text{tpy})(\text{PPP})(\text{OH}_2)](\text{CF}_3\text{SO}_3)_2$ , respectively.

## RESULTS AND DISCUSSION

**X-ray Crystal Structures of 1 and 2.** The ORTEP plots of  $[\text{Ru}(\text{tpy})(\text{PPP})\text{Cl}]^+$  (**1**) and  $[\text{Ru}(\text{tpy})(\text{PPP})(\text{OH}_2)]^{2+}$  (**2**) are shown in Figure 1 (for their crystallographic data, see

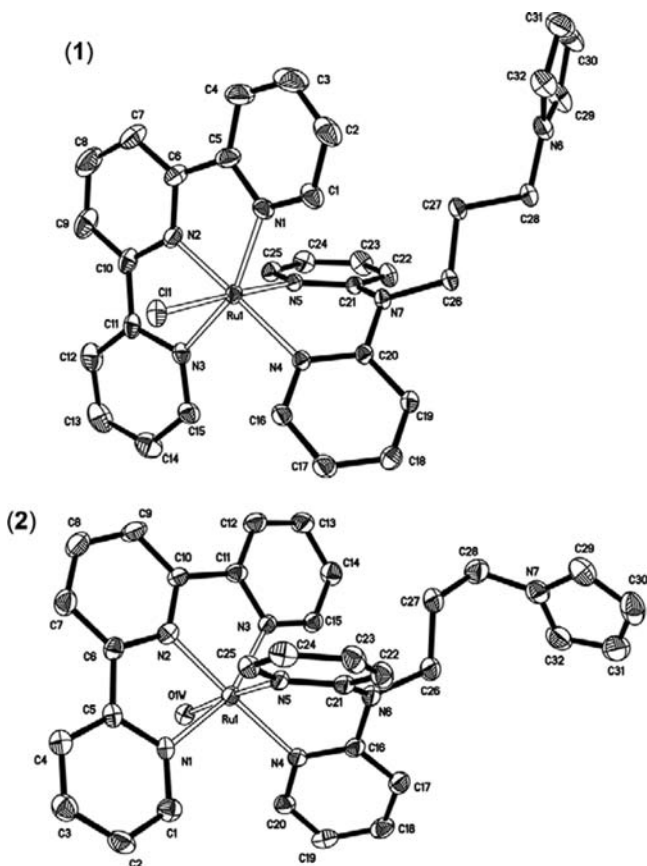
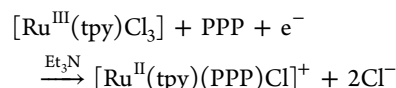


**Figure 1.** ORTEP plots of  $[\text{Ru}(\text{tpy})(\text{PPP})\text{Cl}]^+$  (**1**) and  $[\text{Ru}(\text{tpy})(\text{PPP})(\text{OH}_2)]^{2+}$  (**2**).

Supporting Information, Table S1). These complexes adopt a distorted octahedron structure with the terpyridine ligand coordinated in meridional manner, the PPP ligand in cis position, and chloride or aquo ligand in trans position to one of the PPP nitrogen atoms. The terpyridine ligand is coordinated to the ruthenium center with a bonding angle (N(1)–Ru(1)–N(3)) of approximately  $159^\circ$ . It also exhibits about 0.1 Å shorter Ru–N bonding distance at the central pyridyl ring (Ru(1)–N(2)) than at the two other outer rings, which is typical in ruthenium(II) terpyridine complexes.<sup>18</sup> The Ru–Cl bond distance of 2.4154(9) Å in **1** and Ru–OH<sub>2</sub> bond distance of 2.156(3) Å in **2** are similar to those of 2.4308(2) Å and 2.126(4) Å in  $[\text{Ru}(\text{tpy})(\text{dpa})\text{Cl}]^+$  and  $[\text{Ru}(\text{tpy})(\text{dpa})(\text{OH}_2)]^{2+}$ , respectively.<sup>15</sup> The N(5)–Ru–Cl bond angle of  $178.07(7)^\circ$  in **1** and the N(5)–Ru–O(OH<sub>2</sub>) bond angle of  $177.25(13)^\circ$  in **2** are also similar to those of  $177.49(16)^\circ$  and  $175.38(17)^\circ$  in the dpa analogues.<sup>15</sup> Selected bond distances and angles of **1** and **2** are summarized in Tables S2 and S3, respectively, in the Supporting Information.

**Synthesis and Characterization.** The synthetic procedure for the ruthenium complexes **1–3** is outlined in Scheme 1.

Complex **1** was obtained from the reaction of  $[\text{Ru}(\text{tpy})\text{Cl}_3]$  and PPP in triethylamine with a high yield (93%):



In this reaction, triethylamine acts both as a base and as a reducing agent, assisting the dissociation of  $\text{Cl}^-$  from  $[\text{Ru}(\text{tpy})\text{Cl}_3]$ . This complex was isolated as a perchlorate salt and fully characterized by <sup>1</sup>H NMR, IR, UV–vis, mass spectrometry, and elemental analysis. Further reaction of **1** with silver triflate under dark replaces its chloride ligand with H<sub>2</sub>O, which produces its aquo complex **2** as a triflate salt with 69% yield.

The electronic absorption spectra of complexes **1–3** are shown in Figure 2. The monomeric ruthenium complexes have electronic spectroscopic properties similar to those of their dpa analogues.<sup>15</sup> The replacement of dpa ligand with PPP has little effect on the electronic spectrum. The Ru (*dπ*) to tpy (*π\**) charge transfer band seems to overlap with the Ru (*dπ*) to PPP (*π\**) in each complex, resulting in a very broad absorption band centered at around 500 nm. The Ru (*dπ*) to *π\** MLCT band energy in  $[\text{Ru}^{\text{II}}(\text{tpy})(\text{PPP})\text{X}]^{n+}$  follows the order X =  $\text{Cl}^- < \text{H}_2\text{O} < \text{CH}_3\text{CN}$ , which is in accord with the relative stabilization of the Ru (*dπ*) level by the ligand X.

### Electropolymerization and Electrochemical Studies of 1.

Electrochemical polymerization of the pyrrole tag allows the immobilization of the ruthenium complexes onto the electrode surface. Figure 3a shows typical successive cyclic voltammetric scans of **1** recorded in acetonitrile with 0.1 M tetrabutylammonium perchlorate (TBAP) as the supporting electrolyte. In the first scan from 0.05 to 1.25 V (vs ferrocenium/ferrocene,  $\text{Cp}_2\text{Fe}^{+/0}$ ), an irreversible anodic peak was observed at 0.96 V, which corresponds to the formation of polypyrrole film on the electrode surface. Similar to other N-substituted pyrroles, this peak is suppressed in the subsequent scans as a consequence of the loss in electroactivity of polypyrrole due to fast over-oxidation at this potential.<sup>19</sup> A reversible couple observed at  $E_{1/2} = 0.4$  V vs  $\text{Cp}_2\text{Fe}^{+/0}$  is assigned to the interconversion of  $[\text{Ru}^{\text{III}}(\text{tpy})(\text{PPP})\text{Cl}]^{2+}/[\text{Ru}^{\text{II}}(\text{tpy})(\text{PPP})\text{Cl}]^+$ . The gradual increase in the peak height of this couple in the subsequent scans indicates the build-up of **1** on the electrode surface through the polymerization of its PPP ligand.

With the increasing number of potential sweeps, another reversible couple (**P**<sub>1</sub>) was developed at  $E_{1/2} = 0.82$  V and steadily increased in size. This unexpected couple was absent when the voltammetric scan was switched before the pyrrole polymerization potential (Figure 3b), indicating that this is a new species triggered by the electropolymerization of pyrrole. We assigned **P**<sub>1</sub> to the  $[\text{Ru}^{\text{III}}(\text{tpy})(\text{PPP})(\text{CH}_3\text{CN})]^{3+}/[\text{Ru}^{\text{II}}(\text{tpy})(\text{PPP})(\text{CH}_3\text{CN})]^{2+}$  couple resulting from the replacement of chloride ligand with solvent CH<sub>3</sub>CN for the following reasons. The  $[\text{Ru}(\text{tpy})(\text{PPP})(\text{CH}_3\text{CN})]^{2+}$  complex (**3**), has been prepared for comparison, and the cyclic voltammogram was measured under the same conditions. The observed  $E_{1/2}$  value of **3** is consistent with **P**<sub>1</sub> (Figure S1(a) in the Supporting Information). Figure S1(b) shows the cyclic voltammogram for electropolymerization of **1** in dichloromethane, where **P**<sub>1</sub> is not observed. Although a small couple appeared as a shoulder at  $E_{1/2} = 0.7$  V, this couple is ill-defined and the increment of its height is insignificant. It is believed that dichloromethane cannot play a role as a good coordinating ligand to replace chloride as acetonitrile does. In

Scheme 1. Synthetic Procedure for Ruthenium Complexes

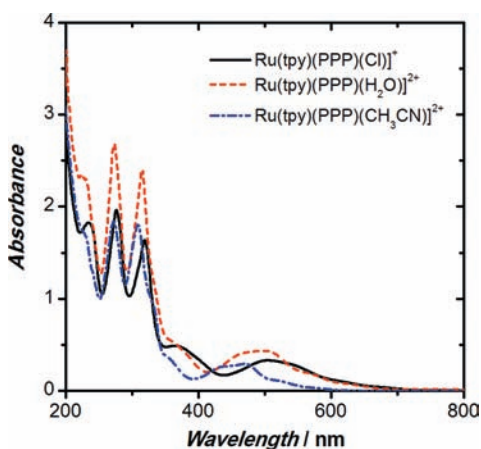
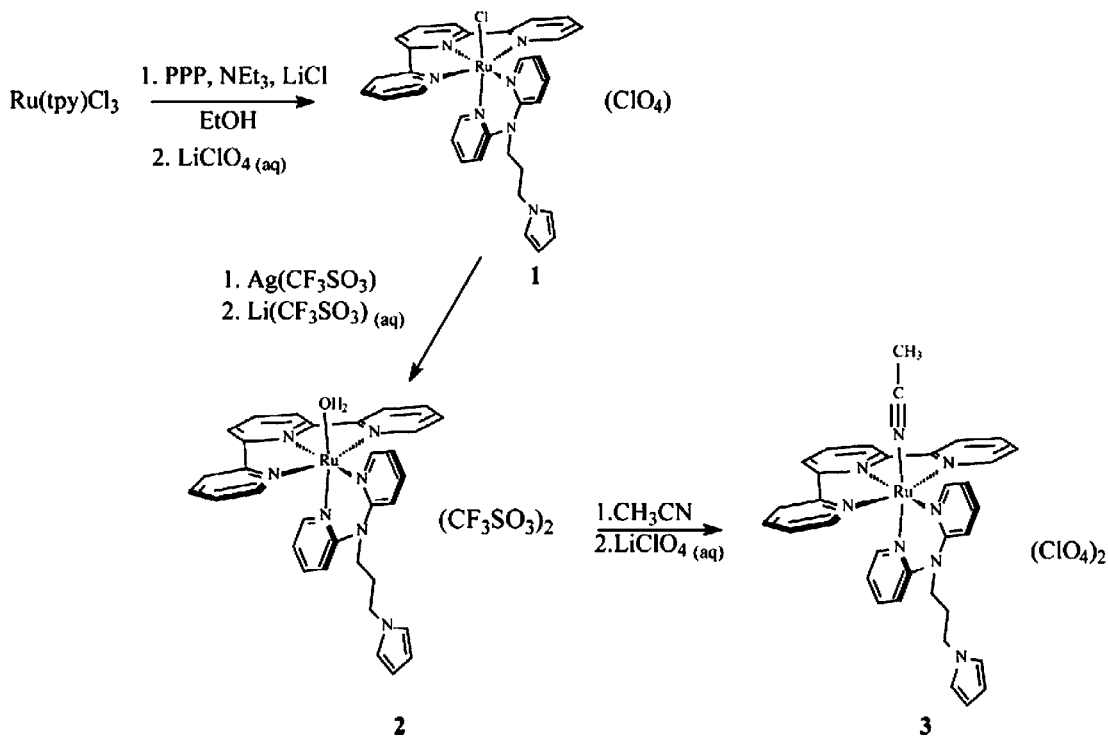


**Figure 2.** Electronic absorption spectra for (a)  $[\text{Ru}(\text{tpy})(\text{PPP})(\text{Cl})]^{2+}$ , (b)  $[\text{Ru}(\text{tpy})(\text{PPP})(\text{H}_2\text{O})]^{2+}$ , and (c)  $[\text{Ru}(\text{tpy})(\text{PPP})(\text{CH}_3\text{CN})]^{2+}$ . Spectra were measured in  $\text{CH}_3\text{CN}$  at room temperature for (a) and (c) and in 0.1 M  $\text{CF}_3\text{SO}_3\text{H}$  for (b).

addition, the higher solubility of polypyrrole film in dichloromethane probably limited its growth on the electrode surface<sup>8a,e</sup> as can be seen from the restrained increase of the  $\text{Ru}^{\text{III}}/\text{Ru}^{\text{II}}$  couple after several scans.

Further investigations on the cause for  $\text{P}_1$  was done with two analogue complexes  $[\text{Ru}(\text{tpy})(\text{dppa})\text{Cl}]^+$  and  $[\text{Ru}(\text{tpy})(\text{dpa})\text{Cl}]^+$ . Both dppa and dpa ligands closely resemble PPP, but they possess no pendant pyrrole moiety. Figure S1(c,d) (Supporting Information) shows successive cyclic voltammograms of  $[\text{Ru}(\text{tpy})(\text{dppa})\text{Cl}]^+$  and  $[\text{Ru}(\text{tpy})(\text{dpa})\text{Cl}]^+$ , respectively, measured under the same conditions as for the electropolymerization of **1**. Both complexes exhibit a  $\text{Ru}^{\text{III}}/\text{Ru}^{\text{II}}$  couple at redox potential close to that for  $[\text{Ru}(\text{tpy})(\text{PPP})\text{Cl}]^+$  ( $E_{1/2} = 0.44$  V for  $[\text{Ru}(\text{tpy})(\text{dppa})\text{Cl}]^+$  and  $E_{1/2} = 0.35$  V for  $[\text{Ru}(\text{tpy})(\text{dpa})\text{Cl}]^+$ ). However, the voltammograms did not

show the appearance of a new couple after a number of potential sweeps indicating that simply cycling between the  $\text{Ru}(\text{II})$  and  $\text{Ru}(\text{III})$  oxidation state would not cause a rapid chloride substitution by acetonitrile. The observation that simply applying the anodic potential cannot induce the chloride substitution from  $[\text{Ru}^{\text{III}}(\text{tpy})(\text{dppa})\text{Cl}]^{2+}$  and  $[\text{Ru}^{\text{III}}(\text{tpy})(\text{dpa})\text{Cl}]^{2+}$  is consistent with the known fact that coordinated halides in  $\text{Ru}(\text{III})$  are less labile than in  $\text{Ru}(\text{II})$  state.<sup>20</sup> In a related experiment where 1  $\mu\text{M}$  of pyrrole was electropolymerized with 0.5 mM of  $[\text{Ru}(\text{tpy})(\text{dpa})\text{Cl}]^+$  as a dopant in acetonitrile, the resulting polypyrrole/ $[\text{Ru}(\text{tpy})(\text{dpa})\text{Cl}]^+$ -modified electrode showed a reversible peak that corresponds to the replacement of chloride by  $\text{CH}_3\text{CN}$  (Figure 4). These results confirm that the pyrrole polymerization is required to induce the chloride substitution in **1**.

Electropolymerization of pyrrole proceeds with the loss of protons, making the local environment highly acidic.<sup>21</sup> Ruthenium(II) and (III) halide complexes were previously reported to undergo acid-catalyzed hydrolysis in aqueous solution.<sup>22</sup> In order to have further insights on how an acidic environment triggers the chloride substitution, we investigated the effect of acidic conditions on the cyclic voltammogram of  $[\text{Ru}^{\text{II}}(\text{tpy})(\text{dpa})\text{Cl}]^+$ . Figure S2 in the Supporting Information shows the cyclic voltammograms of  $[\text{Ru}^{\text{II}}(\text{tpy})(\text{dpa})\text{Cl}]^+$  in acetonitrile at different time elapses after the addition of 0.1 M triflic acid. Under this acidic condition, the  $[\text{Ru}^{\text{III}}(\text{tpy})(\text{dpa})\text{Cl}]^{2+}/[\text{Ru}^{\text{II}}(\text{tpy})(\text{dpa})\text{Cl}]^+$  couple was shifted by 50 mV in the cathodic direction. After 10 min in the presence of 0.1 M acid, the redox peak for  $[\text{Ru}^{\text{III}}(\text{tpy})(\text{dpa})\text{Cl}]^{2+}/[\text{Ru}^{\text{II}}(\text{tpy})(\text{dpa})\text{Cl}]^+$  decreased and a new couple appeared at around 0.8 V which corresponds to the  $\text{CH}_3\text{CN}$ -substituted complex. This switch of peak height further developed with time. Although the presence of 0.1 M acid facilitated chloride substitution in the electro-oxidation of  $[\text{Ru}^{\text{II}}(\text{tpy})(\text{dpa})\text{Cl}]^+$ , the rate of substitution was much slower compared to when pyrrole electropolymerization

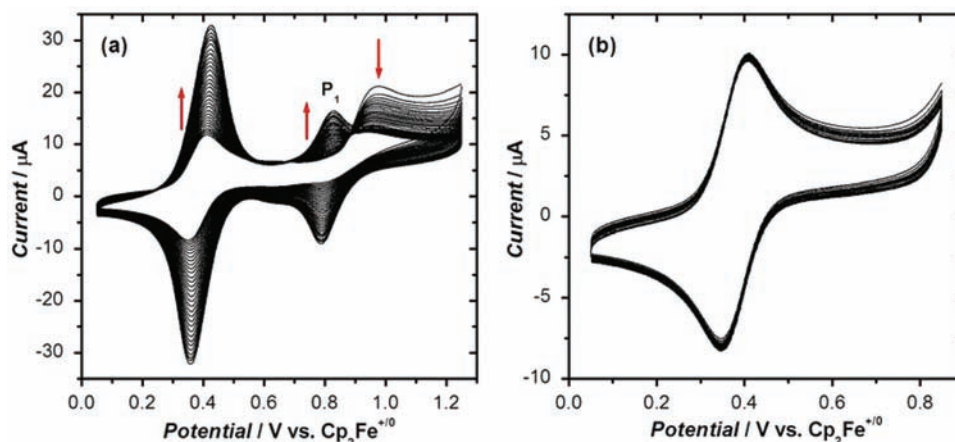


Figure 3. Successive cyclic voltammograms of 0.5 mM  $[\text{Ru}(\text{tpy})(\text{PPP})\text{Cl}]^+$  in  $\text{CH}_3\text{CN}$  with 0.1 M TBAP. Scan rate:  $100 \text{ mV}\cdot\text{s}^{-1}$ .

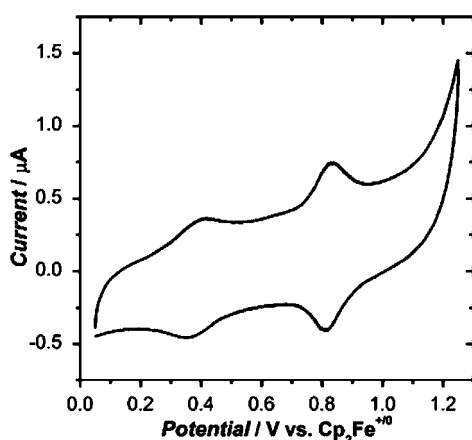


Figure 4. Cyclic voltammogram of polypyrrole/ $[\text{Ru}(\text{tpy})(\text{dpa})\text{Cl}]^+$ -modified glassy carbon electrode measured in  $\text{CH}_3\text{CN}$  with 0.1 M TBAP. The polypyrrole film was deposited by repeated potential scans from 0.05 to 1.25 V in 0.1 M TBAP  $\text{CH}_3\text{CN}$  solution in the presence of 0.5 mM  $[\text{Ru}(\text{tpy})(\text{dpa})\text{Cl}]^+$ . The concentration of pyrrole was 1  $\mu\text{M}$ .

was involved. It is probably due to insufficient acidity since the local environment during pyrrole polymerization was much more acidic. Use of higher acid concentration accelerated the

rate of chloride substitution, but a new couple was also developed which might be due to a triflate-substituted complex.

#### Electropolymerization and Electrochemical Studies of 2.

Although there have been many studies on the electropolymerization of ruthenium aquo complexes with pyrrole-containing ligands in nonaqueous solvents,<sup>6b,8c,d,11b</sup> direct electropolymerization in aqueous medium has not been reported to the best of our knowledge, probably due to the insolubility of those complexes in aqueous medium. The fact that **2** is soluble in water allowed the investigation of its electrochemistry in aqueous medium. Figure 5a shows the cyclic voltammogram for electropolymerization of complex **2** onto a glassy carbon electrode in 0.1 M  $\text{HClO}_4$  by repetitive scans from 0.4 to 1.1 V (vs SCE). In the first cycle, an anodic peak was observed at  $E_{p,a} = 0.86 \text{ V}$ , which corresponds to the oxidation of Ru(II) to Ru(III). An irreversible peak observed at  $E_{p,a} = 0.98 \text{ V}$  was assigned to the oxidation of the pyrrolic units. The subsequent cycling of the potential revealed two growing reversible couples, one at  $E_{1/2} = 0.8 \text{ V}$  and the other at  $E_{1/2} = 0.89 \text{ V}$ . Similar to the other ruthenium(II) aquo complexes, these two couples are assigned to the  $\text{Ru}^{\text{III}}/\text{Ru}^{\text{II}}$  and  $\text{Ru}^{\text{IV}}/\text{Ru}^{\text{III}}$  couples, respectively. The polymer film grew on the electrode surface with the increase in number of scans. The resulting poly $[\text{Ru}(\text{tpy})(\text{PPP})(\text{OH}_2)]^{n+}$  film was stable, and the two reversible couples were still observable when the poly $[\text{Ru}(\text{tpy})(\text{PPP})(\text{OH}_2)]^{n+}$ -modified electrode was transferred to

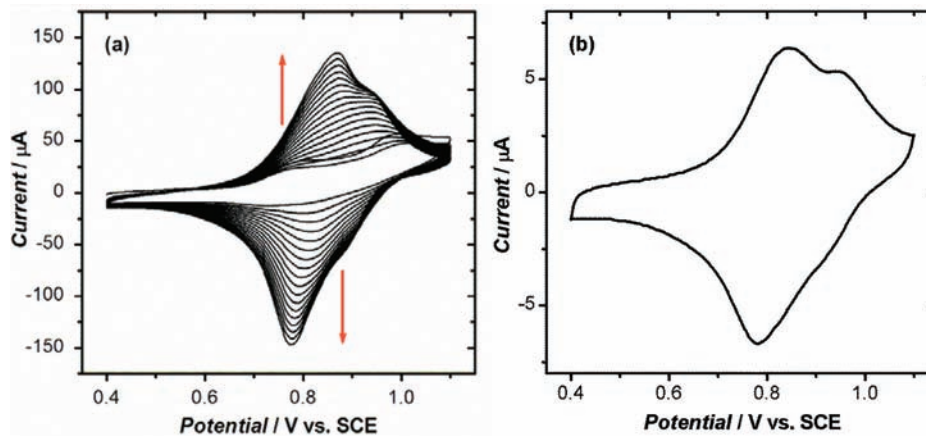
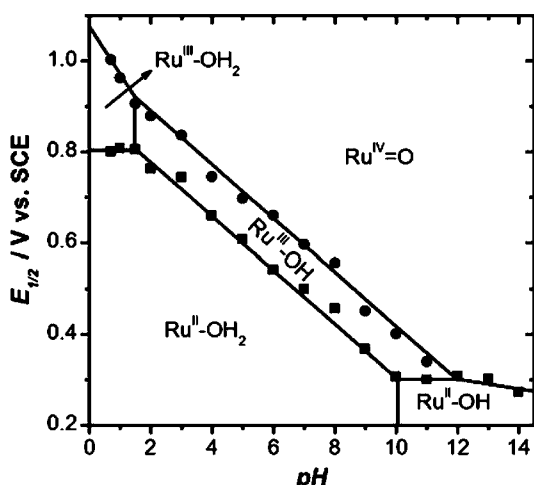


Figure 5. Cyclic voltammograms of (a) 0.5 mM  $[\text{Ru}(\text{tpy})(\text{PPP})(\text{OH}_2)]^{2+}$  and (b) poly $[\text{Ru}(\text{tpy})(\text{PPP})(\text{OH}_2)]^{n+}$  films on a glassy carbon electrode. Both were measured in 0.1 M  $\text{HClO}_4$  at scan rates of (a)  $100 \text{ mV}\cdot\text{s}^{-1}$  and (b)  $20 \text{ mV}\cdot\text{s}^{-1}$ .

blank electrolytes of a wide range of pH ( $0.5 < \text{pH} < 14$ , Figure 5b). The porous morphology of the poly[Ru(tpy)(PPP)(OH<sub>2</sub>)]<sup>n+</sup>(ClO<sub>4</sub>)<sub>n</sub> film revealed by SEM (Figure S3, Supporting Information) is consistent with other previously reported polypyrrole films.<sup>23</sup>

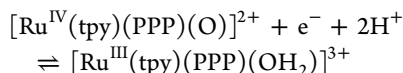
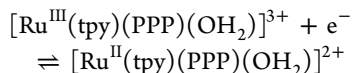
Figure 6 shows the Pourbaix diagram where the  $E_{1/2}$  values of both the Ru<sup>III</sup>/Ru<sup>II</sup> and Ru<sup>IV</sup>/Ru<sup>III</sup> couples are plotted against



**Figure 6.** Pourbaix diagram of poly[Ru(tpy)(PPP)(OH<sub>2</sub>)]<sup>n+</sup> film on a glassy carbon electrode.

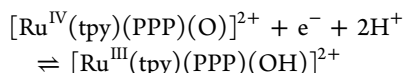
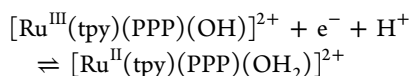
pH. Under strong acidic conditions ( $\text{pH} < 1.7$ ), the  $E_{1/2}$  value for the Ru<sup>III</sup>/Ru<sup>II</sup> couple is independent of pH, whereas that for the Ru<sup>IV</sup>/Ru<sup>III</sup> couple changes with a slope of  $-118 \text{ mV/pH}$ .

$\text{pH} < 1.7$



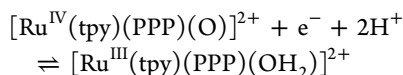
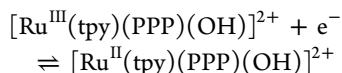
From pH 1.7 to 10, the slopes for both the Ru<sup>III</sup>/Ru<sup>II</sup> and Ru<sup>IV</sup>/Ru<sup>III</sup> couples in the Pourbaix diagram are equal to  $-60 \text{ mV/pH}$ , indicative of one-proton, one-electron processes.

$1.7 < \text{pH} < 10$



At  $\text{pH} > 10$ , the slope for the Ru<sup>III</sup>/Ru<sup>II</sup> couple in the Pourbaix diagram becomes zero, whereas that for the Ru<sup>IV</sup>/Ru<sup>III</sup> couple remains at  $-60 \text{ mV/pH}$ .

$\text{pH} > 10$



Based on the above results, the  $\text{pK}_a$  values for [Ru<sup>III</sup>(tpy)(PPP)(OH<sub>2</sub>)]<sup>3+</sup> and [Ru<sup>II</sup>(tpy)(PPP)(OH<sub>2</sub>)]<sup>2+</sup> were estimated to be 1.7 and 10, respectively. The estimated  $\text{pK}_a$  values are close to those of 1.7 and 9.7 for [Ru<sup>III</sup>(tpy)(bpy)(OH<sub>2</sub>)]<sup>3+</sup> and [Ru<sup>II</sup>(tpy)(bpy)(OH<sub>2</sub>)]<sup>2+</sup> and 1.2 and 11.1 for [Ru<sup>III</sup>(bpea)(bpy)(OH<sub>2</sub>)]<sup>3+</sup> and [Ru<sup>II</sup>(bpea)(bpy)(OH<sub>2</sub>)]<sup>2+</sup> (bpea = *N,N*-bis(2-pyridylmethyl)ethylamine, bpy = 2,2'-bipyridine),<sup>24</sup> respectively, in solution, indicating the polypyrrole film does not exert much effect on the  $\text{pK}_a$  of the ruthenium complex. The formation of [Ru(tpy)(PPP)(O)]<sup>2+</sup> upon the oxidation of [Ru(tpy)(PPP)(OH<sub>2</sub>)]<sup>2+</sup> was supported by the observation of an IR absorption peak at  $790 \text{ cm}^{-1}$  assigned to  $\nu(\text{Ru}^{\text{IV}}=\text{O})$ <sup>25</sup> when [Ru(tpy)(PPP)(OH<sub>2</sub>)]<sup>2+</sup> was oxidized by Ce<sup>IV</sup> (Figure S4, Supporting Information). Oxidation of [Ru(tpy)(PPP)(<sup>18</sup>OH<sub>2</sub>)]<sup>2+</sup> prepared by stirring [Ru(tpy)(PPP)(OH<sub>2</sub>)]<sup>2+</sup> in H<sub>2</sub><sup>18</sup>O with Ce<sup>IV</sup> resulted in the formation of Ru<sup>IV</sup>=<sup>18</sup>O species which exhibited an IR band at  $753 \text{ cm}^{-1}$ .

We noted that the polymerization of pyrrole units, as well as the appearance of the Ru<sup>IV</sup>/Ru<sup>III</sup> couple of poly[Ru<sup>II</sup>(tpy)(PPP)(OH<sub>2</sub>)]<sup>n+</sup> film, is dependent on the electrolyte used. Generally, in the presence of perchlorate anion, the growth of the polypyrrole film is facilitated and the Ru<sup>IV</sup>/Ru<sup>III</sup> couple in the resulting polymer film is clearly defined. For example, when 0.1 M HClO<sub>4</sub> was replaced by other acids such as 0.1 M HBF<sub>4</sub>, CF<sub>3</sub>SO<sub>3</sub>H, CF<sub>3</sub>COOH, or H<sub>2</sub>SO<sub>4</sub> as an alternative electrolyte, not only was a retardation on the growth of the polymer film observed, but the Ru<sup>IV</sup>/Ru<sup>III</sup> couple also became ill-defined. The growth of the polymer film is also facilitated by another bulky anion sodium dodecyl sulfate (SDS), except that an additional shoulder caused by the substitution of aqua ligand with SDS appeared at 0.82 V. The above observations are consistent with previous reports that bulky anions such as perchlorate or SDS are required to produce a conductive and thick polypyrrole film by electropolymerization and these bulky anions will remain as dopants inside the polymer.<sup>26</sup> As the film grew, the size of the Ru<sup>III</sup>/Ru<sup>II</sup> couple ( $E_{1/2} = 0.8 \text{ V vs SCE}$  at pH 1) of poly[Ru(tpy)(PPP)(OH<sub>2</sub>)]<sup>n+</sup> increased accordingly, whereas the growth of the Ru<sup>IV</sup>/Ru<sup>III</sup> couple ( $E_{1/2} = 0.89 \text{ V vs SCE}$  at pH 1) leveled off after the film had reached a certain thickness. These films were deposited from a freshly prepared 0.5 mM [Ru<sup>II</sup>(tpy)(PPP)(OH<sub>2</sub>)]<sup>2+</sup> in 0.1 M HClO<sub>4</sub> solution and transferred to a blank electrolyte of 0.1 M HClO<sub>4</sub> for the cyclic voltammetric studies. Figure 7 shows the cyclic voltammograms and differential pulse voltammograms measured from poly[Ru<sup>II</sup>(tpy)(PPP)(OH<sub>2</sub>)]<sup>n+</sup>-modified electrodes of four different thicknesses. When the polymer film was only very thin, the size of the Ru<sup>IV</sup>/Ru<sup>III</sup> and the Ru<sup>III</sup>/Ru<sup>II</sup> couples are similar. The size of the Ru<sup>III</sup>/Ru<sup>II</sup> couple progressively increased with the number of potential scans, indicating the build-up of ruthenium complexes in the thicker polymer film. However, the size of the Ru<sup>IV</sup>/Ru<sup>III</sup> couple leveled off quickly as the film grew in thickness, indicating the hindrance of the formation of Ru<sup>IV</sup>=O species in the thicker polymer films. The electrochemical formation of Ru<sup>IV</sup>=O from Ru<sup>III</sup>-OH<sub>2</sub> or Ru<sup>III</sup>-OH is a kinetically slow process and likely to occur via a concerted proton-electron transfer mechanism.<sup>27</sup> The oxidation of Ru<sup>III</sup>-OH<sub>2</sub> or Ru<sup>III</sup>-OH to Ru<sup>IV</sup>=O probably occurs via the formation of a preassociated complex with a base forming hydrogen-bonding with the hydrogen on the aquo or hydroxo ligand of the Ru(III) center.<sup>27</sup> The thickening and cross-linking of the polymer film might hinder the formation of

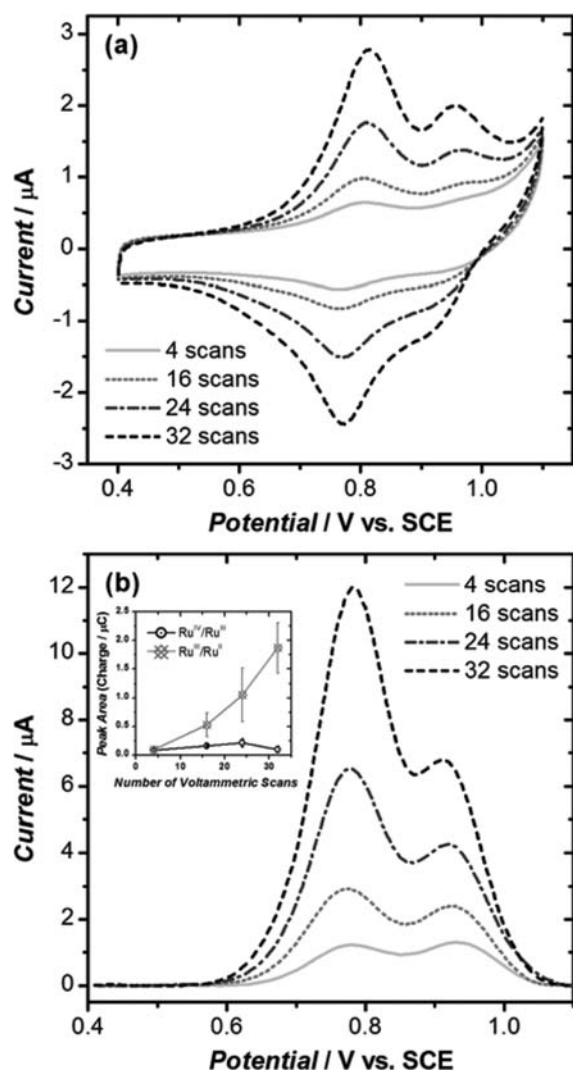


**Figure 7.** (a) Cyclic voltammograms and (b) differential pulse voltammograms of four poly[ $\text{Ru}^{\text{II}}(\text{tpy})(\text{PPP})(\text{OH}_2)]^{n+}$ -modified electrodes of different film thicknesses measured in 0.1 M  $\text{HClO}_4$ . The poly[ $\text{Ru}^{\text{II}}(\text{tpy})(\text{PPP})(\text{OH}_2)]^{n+}$ -modified electrodes were prepared by different number of potential scans in 0.5 mM [ $\text{Ru}^{\text{II}}(\text{tpy})(\text{PPP})(\text{OH}_2)]^{2+}$  + 0.1 M  $\text{HClO}_4$ . The inset in (b) indicates charges associated with the  $\text{Ru}^{\text{IV}}/\text{Ru}^{\text{III}}$  and  $\text{Ru}^{\text{III}}/\text{Ru}^{\text{II}}$  couples from the poly[ $\text{Ru}^{\text{II}}(\text{tpy})(\text{PPP})(\text{OH}_2)]^{n+}$ -modified electrodes. Scan rates: (a) 20  $\text{mV}\cdot\text{s}^{-1}$  and (b) 50  $\text{mV}\cdot\text{s}^{-1}$ .

this preassociated complex. For examples, ruthenium aquo complexes further away from the electrode surface would not be able to interact with the quinone-like functional groups on the carbon electrode,<sup>28</sup> and the increase in cross-linking of the polymer backbone would also hinder the preassociation with other bases.

The formation of  $\text{Ru}^{\text{IV}}=\text{O}$  species was also supported by the electrocatalytic property of the polymer film. A polymer film was formed on the glassy carbon electrode surface by cycling the potential between 0.4 and 1.1 V (vs SCE) 32 times in 0.1 M  $\text{HClO}_4$  solution containing 0.5 mM complex 2, at a scan rate of 100  $\text{mV}\cdot\text{s}^{-1}$ . In the presence of 10 mM benzyl alcohol, an increase in anodic current was observed at the potential where  $\text{Ru}^{\text{III}}-\text{OH}_2$  is oxidized to  $\text{Ru}^{\text{IV}}=\text{O}$  (Figure 8). Constant potential electrolysis at 0.9 V for 14 h with a carbon felt electrode coated with a poly[ $\text{Ru}^{\text{II}}(\text{tpy})(\text{PPP})(\text{OH}_2)]^{n+}$  film containing  $8.0 \times 10^{-8}$  mol of ruthenium centers and in the

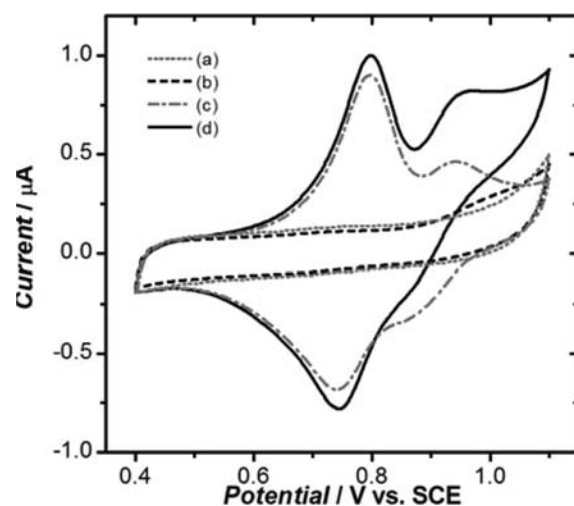


**Figure 8.** Cyclic voltammograms of a bare (a and b) and a poly[ $\text{Ru}(\text{tpy})(\text{PPP})(\text{OH}_2)]^{n+}$ -coated (c and d) glassy carbon electrode measured in 0.1 M  $\text{HClO}_4$ . (b) and (d) were measured in the presence of 10 mM benzyl alcohol. Scan rate: 5  $\text{mV}\cdot\text{s}^{-1}$ .

presence of 20 mM benzyl alcohol resulted in the production of  $\sim 5$  mM of benzaldehyde as identified by gas chromatography. This conversion corresponds to 430 redox cycles of the metal centers and a current efficiency of 59%. The current efficiency is comparable to a previous report in which a similar ruthenium complex [ $\text{Ru}(\text{bpea-pyr})(\text{bpy-pyr})(\text{OH}_2)]^{2+}$  (bpea-pyr = bis-pyridin-2-ylmethyl-(3-pyrrol-1-yl-propyl)amine, bpy-pyr = 4-methyl-4'-(4-pyrrol-1-yl-butyl)-[2,2']-bipyridine) was polymerized in dichloromethane and used for electrocatalysis of benzyl alcohol oxidation.<sup>11b</sup>

## CONCLUSION

In summary, we have synthesized several new ruthenium complexes, [ $\text{Ru}(\text{tpy})(\text{PPP})\text{Cl}]\text{ClO}_4$ , [ $\text{Ru}(\text{tpy})(\text{PPP})(\text{OH}_2)]-(\text{CF}_3\text{SO}_3)_2$ , and [ $\text{Ru}(\text{tpy})(\text{PPP})(\text{CH}_3\text{CN})](\text{ClO}_4)_2$ , that contain an electropolymerizable pyrrole-tagged ligand *N*-(3-bis(2-pyridyl)aminopropyl)pyrrole (PPP), and have successfully anchored them onto carbon electrodes via anodic oxidation of the pyrrole groups. The resulting polymer films are stable and highly electroactive. The protons released during polypyrrole formation of [ $\text{Ru}(\text{tpy})(\text{PPP})\text{Cl}]^+$  were found to be responsible for the chloride substitution with solution  $\text{CH}_3\text{CN}$ . The use of PPP ligand allowed the polymerization of [ $\text{Ru}(\text{tpy})(\text{PPP})(\text{OH}_2)]^{2+}$  in aqueous medium and the observation of the formation of [ $\text{Ru}^{\text{IV}}=\text{O}]^{2+}$  in the polypyrrole film. The slow kinetics in the formation of  $\text{Ru}^{\text{IV}}=\text{O}$  in the polymer film is attributed to the hindrance of the formation of preassociated complexes essential for concerted proton-electron transfer reaction by the polymer. The poly[ $\text{Ru}(\text{tpy})(\text{PPP})(\text{OH}_2)]^{n+}$ -modified electrode is catalytically active toward the electro-oxidation of benzyl alcohol.

## ASSOCIATED CONTENT

### Supporting Information

X-ray crystallographic data for complexes 1 and 2 in CIF format, crystal data, refinement details, selected bond distances and angles, and electronic absorption spectroscopic data for complexes 1 and 2, cyclic voltammograms of 3 and analogues of 1, SEM image of poly[ $\text{Ru}(\text{tpy})(\text{PPP})(\text{OH}_2)]^{n+}$ , IR spectra of complex 2, [ $\text{Ru}(\text{tpy})(\text{PPP})(^{16}\text{O})]^{2+}$ , and [ $\text{Ru}(\text{tpy})(\text{PPP})-$

( $^{18}\text{O}$ ) $^{2+}$ . This material is available free of charge via the Internet at <http://pubs.acs.org>.

## AUTHOR INFORMATION

### Corresponding Author

\*E-mail: [bckywong@polyu.edu.hk](mailto:bckywong@polyu.edu.hk). Fax: +852 2364 9932. Tel: +852 3400 3977.

### Notes

The authors declare no competing financial interest.

## ACKNOWLEDGMENTS

We acknowledge the support from The Hong Kong Polytechnic University, the Research Grants Council (Grant PolyU 5015/07P), and the Innovation and Technology Commission.

## REFERENCES

- (1) (a) Murray, R. W. Ed. *Molecular Design of Electrode Surfaces*; John Wiley: New York, 1992. (b) Ulman, A. *An Introduction to Ultrathin Organic Films: From Langmuir-Blodgett to Self-Assembly*; Academic Press: New York, 1991.
- (2) (a) Zhou, J.; Wang, E. *Electroanalysis* **1994**, *6*, 29–35. (b) Zinger, B.; Miller, L. L. *J. Electroanal. Chem. Interfacial Electrochem.* **1984**, *181*, 153–172.
- (3) Chou, H. A.; Zavitz, D. H.; Ovadia, M. *Biosens. Bioelectron.* **2003**, *18*, 11–21.
- (4) Chen, J.; Reed, M. A.; Rawlett, A. M.; Tour, J. M. *Science* **1999**, *286*, 1550–1552.
- (5) Diaz, A. F.; Kanazawa, K. K.; Gardini, G. P. *J. Chem. Soc., Chem. Commun.* **1979**, 635–636.
- (6) (a) Leider, C. R.; Murray, R. W. *J. Am. Chem. Soc.* **1984**, *106*, 1606–1614. (b) Guadalupe, A. R.; Chen, X.; Sullivan, B. P.; Meyer, T. *J. Inorg. Chem.* **1993**, *32*, 5502–5512. (c) Pickup, P. G. *J. Mater. Chem.* **1999**, *9*, 1641–1653. (d) Potts, K. T.; Usifer, D. A.; Guadalupe, A.; Abruna, H. D. *J. Am. Chem. Soc.* **1987**, *109*, 3961–3967. (e) Gould, S.; Strouse, G. F.; Meyer, T. J.; Sullivan, B. P. *Inorg. Chem.* **1991**, *30*, 2942–2949. (f) Horwitz, C. P.; Zuo, Q. *Inorg. Chem.* **1992**, *31*, 1607–1613. (g) Andrieux, C. P.; Haas, O.; Saveant, J. M. *J. Am. Chem. Soc.* **1986**, *108*, 8175–8182. (h) Zhang, H.; Murray, R. W. *J. Am. Chem. Soc.* **1993**, *115*, 2335–2340.
- (7) (a) Deronzier, A.; Moutet, J. C. *Acc. Chem. Res.* **1989**, *22*, 249–255. (b) Deronzier, A.; Moutet, J. C. *Coord. Chem. Rev.* **1996**, *147*, 339–371.
- (8) (a) Cosnier, S.; Deronzier, A.; Moutet, J. C. *J. Electroanal. Chem. Interfacial Electrochem.* **1985**, *193*, 193–204. (b) De Giovanni, W. F.; Deronzier, A. *J. Chem. Soc., Chem. Commun.* **1992**, 1461–1463. (c) De Giovanni, W. F.; Deronzier, A. *J. Electroanal. Chem.* **1992**, *337*, 285–298. (d) Collomb-Dunand-Sauthier, M.-N.; Deronzier, A.; Bozec, H. L.; Navarro, M. *J. Electroanal. Chem.* **1996**, *410*, 21–29. (e) Collomb-Dunand-Sauthier, M.-N.; Deronzier, A.; Navarro, M. *Chem. Commun.* **1996**, 2165–2166.
- (9) (a) Cosnier, S.; Deronzier, A.; Moutet, J. C. *J. Mol. Catal.* **1988**, *45*, 381–391. (b) Cosnier, S.; Deronzier, A.; Moutet, J. C. *J. Electroanal. Chem. Interfacial Electrochem.* **1986**, *207*, 315–321. (c) Cosnier, S.; Deronzier, A.; Moutet, J. C. *New J. Chem.* **1990**, *14*, 831–839.
- (10) (a) Deronzier, A.; Devaux, R.; Limosin, D.; Latour, J. M. *J. Electroanal. Chem.* **1992**, *324*, 325–337. (b) Collomb-Dunand-Sauthier, M.-N.; Deronzier, A. *J. Electroanal. Chem.* **1995**, *391*, 211–214.
- (11) (a) Romero, I.; Rodriguez, M.; Llobet, A.; Collomb-Dunand-Sauthier, M.-N.; Deronzier, A.; Parella, T.; Stoekli-Evans, H. *J. Chem. Soc., Dalton Trans.* **2000**, 1689–1694. (b) Rodriguez, M.; Romero, I.; Sens, C.; Llobet, A.; Deronzier, A. *Electrochim. Acta* **2003**, *48*, 1047–1054.
- (12) Cheung, K.-C.; Guo, P.; So, M.-H.; Lee, L. Y. S.; Ho, K.-P.; Wong, W.-L.; Lee, K.-H.; Wong, W.-T.; Zhou, Z.-Y.; Wong, K.-Y. *J. Organomet. Chem.* **2009**, *694*, 2842–2845.
- (13) (a) Moyer, B. A.; Thompson, M. S.; Meyer, T. J. *J. Am. Chem. Soc.* **1980**, *102*, 2310–2312. (b) Samuels, G. J.; Meyer, T. J. *J. Am. Chem. Soc.* **1981**, *103*, 307–312. (c) Thompson, M. S.; De Giovanni, W. F.; Moyer, B. A.; Meyer, T. J. *J. Org. Chem.* **1984**, *49*, 4972–4977. (d) Grover, N.; Gupta, N.; Singh, P.; Thorp, H. H. *Inorg. Chem.* **1992**, *31*, 2014–2020. (e) Moss, J. A.; Leasure, R. M.; Meyer, T. J. *Inorg. Chem.* **2000**, *39*, 1052–1058. (f) Ho, C.; Che, C. M.; Lau, T. C. *J. Chem. Soc., Dalton Trans.* **1990**, 967–970.
- (14) Takeuchi, K. J.; Thompson, M. S.; Pipes, D. W.; Meyer, T. J. *Inorg. Chem.* **1984**, *23*, 1845–1851.
- (15) Chanda, N.; Mobin, S. M.; Puranik, V. G.; Datta, A.; Niemeyer, M.; Lahiri, G. K. *Inorg. Chem.* **2004**, *43*, 1056–1064.
- (16) Mock, C.; Puscasu, I.; Rauterkus, M. J.; Tallen, G.; Wolff, J. E. A.; Krebs, B. *Inorg. Chim. Acta* **2001**, *319*, 109–116.
- (17) Muller, P.; Herst-Irmer, R.; Spek, A.; Schneider, T. R.; Sawaya, M. R. *Crystal structure refinement: a crystallographer's guide to SHELXL*; Oxford University Press: Oxford, UK, 2006.
- (18) (a) Adcock, P. A.; Keene, F. R.; Smythe, R. S.; Snow, M. R. *Inorg. Chem.* **1984**, *23*, 2336–43. (b) Spek, A. L.; Gerli, A.; Reedijk, J. *Acta Crystallogr., Sect. C: Cryst. Struct. Commun.* **1994**, *C50*, 394–397. (c) Hecker, C. R.; Fanwick, P. E.; McMillin, D. R. *Inorg. Chem.* **1991**, *30*, 659–666. (d) Leising, R. A.; Kubow, S. A.; Churchill, M. R.; Buttrey, L. A.; Ziller, J. W.; Takeuchi, K. J. *Inorg. Chem.* **1990**, *29*, 1306–1312. (e) Thummel, R. P.; Jahng, Y. *Inorg. Chem.* **1986**, *25*, 2527–2534. (f) Gupta, N.; Grover, N.; Neyhart, G. A.; Liang, W.; Singh, P.; Thorp, H. H. *Angew. Chem., Int. Ed.* **1992**, *31*, 1048–1050. (g) Mondal, B.; Puranik, V. G.; Lahiri, G. K. *Inorg. Chem.* **2002**, *41*, 5831–5836. (h) Catalano, V. J.; Heck, R. A.; Ohman, A.; Hill, M. G. *Polyhedron* **2000**, *19*, 1049–1055.
- (19) (a) Cosnier, S.; Deronzier, A.; Roland, J. F. *J. Electroanal. Chem.* **1990**, *285*, 133–147. (b) Deiss, E.; Haas, O.; Daul, C. *J. Electroanal. Chem.* **1992**, *337*, 299–324. (c) Deronzier, A.; Essakalli, M. *J. Chem. Soc., Chem. Commun.* **1990**, 242–244.
- (20) Poon, C. K.; Che, C. M.; Kan, Y. P. *J. Chem. Soc., Dalton Trans.* **1980**, 128–133.
- (21) Street, G. B. In *Handbook of Conducting Polymers*; Skotheim, T. A., Ed.; Marcel Dekker: New York, 1986; Vol. 1, p 265.
- (22) (a) Broomhead, J. A.; Basolo, F.; Pearson, R. G. *Inorg. Chem.* **1964**, *3*, 826–832. (b) Ferreira, K. Q.; Doro, F. G.; Tfouni, E. *Inorg. Chim. Acta* **2003**, *355*, 205–212.
- (23) Chen, W. C.; Wen, T. C. *J. Power Sources* **2003**, *117*, 273–282.
- (24) Rodriguez, M.; Romero, I.; Llobet, A.; Deronzier, A.; Biner, M.; Parella, T.; Stoekli-Evans, H. *Inorg. Chem.* **2001**, *40*, 4150–4156.
- (25) (a) Griffith, W. P. *Transition Met. Chem.* **1990**, *15*, 251–256. (b) Che, C.-M.; Ho, C.; Lau, T.-C. *J. Chem. Soc., Dalton Trans.* **1991**, 1901–1907.
- (26) (a) Peres, R. C. D.; Pernaut, J. M.; De Paoli, M. A. *Synth. Met.* **1989**, *28*, 59–64. (b) Atanasoska, L.; Naoi, K.; Smyrl, W. H. *Chem. Mater.* **1992**, *4*, 988–994. (c) Shimidzu, T.; Ohtani, A.; Lyoda, T.; Honda, K. *J. Electroanal. Chem.* **1987**, *224*, 123–135. (d) Reghu, M.; Subramanyan, S. V.; Chatterjee, S. *Phys. Rev. B* **1991**, *43*, 4236–4243.
- (27) (a) Huyuh, M. H. V.; Meyer, T. J. *Chem. Rev.* **2007**, *107*, 5004–5064. (b) Meyer, T. J.; Huynh, M. H. V. *Inorg. Chem.* **2003**, *42*, 8140–8160.
- (28) (a) Cabaniss, G. E.; Diamantis, A. A.; Murphy, W. R., Jr.; Linton, R. W.; Meyer, T. J. *J. Am. Chem. Soc.* **1985**, *107*, 1845–1853. (b) Xu, J.; Chen, Q.; Swain, G. M. *Anal. Chem.* **1998**, *70*, 3146–3154.